CURRENT NOISE PARAMETERS DERIVED FROM VOLTAGE NOISE AND IMPEDANCE IN EMBRYONIC HEART CELL AGGREGATES

JOHN R. CLAY, LOUIS J. DEFELICE, AND ROBERT L. DEHAAN, *Department of Anatomy, Emory University, Atlanta, Georgia 30322 U.S.A.*

ABSTRACT We have recorded membrane impedance and voltage noise in the pacemaker range of potentials (−70 to −59 mV) from spheroidal aggregates of 7-d embryonic chick ventricle cells made quiescent by exposure to tetrodotoxin in medium containing 4.5 mM K^+. The input capacitance is proportional to aggregate volume and therefore to total membrane area. The specific membrane capacitance is 1.24 $\mu F/cm^2$. The input resistance at constant potential is inversely proportional to aggregate volume and therefore to total membrane area. The specific membrane resistance is 18 $k\Omega \cdot cm^2$ at −70 mV and increases to 81 $k\Omega \cdot cm^2$ at −59 mV. The RC time constant is 22 ms at −70 mV and increases to 146 ms at −59 mV. The aggregate transmembrane small-signal impedance can be represented by a parallel RC circuit itself in parallel with an inductive branch consisting of a resistor (r_L) and an inductor (L) in series. The time constant of the inductive branch (L/r_L) is 340 ms, and is only weakly dependent on potential. Correlation functions of aggregate voltage noise and the impedance data were modeled by a population of channels with simple open-close kinetics. The time constant of a channel (τ_s) derived from the noise analysis is 300 ms. The low frequency limit of the pacemaker current noise ($S_I[0]$), derived from the voltage noise and impedance, increases from 10^{-20} $A^2/Hz \cdot cm^2$ at −67 mV to 10^{-19} $A^2/Hz \cdot cm^2$ at −61 mV.

INTRODUCTION

The primary aim of the present study was to determine the current noise characteristics of a tissue culture model of the heart cell membrane from measurements of small-signal impedance and inherent voltage noise. We have shown that such a model is provided by spheroidal aggregates of electrically coupled embryonic heart cells (DeHaan and Sachs, 1972; Sachs and DeHaan, 1973; DeFelice and DeHaan, 1977). To interpret the relationship between current noise and voltage it was necessary to determine the extent to which the membrane of all cells in an aggregate is charged simultaneously by a current pulse. Previous studies have shown that these preparations approach a state of internal voltage homogeneity at potentials near rest for low frequency signals (DeHaan and Fozzard, 1975; DeFelice and DeHaan, 1977; Nathan and DeHaan, 1979). In the present work we have used an indirect method for investigating the degree of uniformity of the transmembrane potential by measuring membrane capacitance and resistance as a function of aggregate size.

The principal results of the impedance and noise analysis are that (*a*) for small current steps that produce voltage responses having a frequency content <10 Hz, the total membrane area is charged simultaneously and without appreciable decrement; (*b*) membrane slope resistance, as measured from step responses, increases with depolarization at potentials near rest; and (*c*) current noise amplitude also increases with depolarization in the same voltage

range. These results provide constraints on the voltage- and time-dependent conductances that may underlie the measured impedance and voltage noise. Several alternative models are presented in the Discussion.

METHODS

Tissue Preparation

The apical portions of heart ventricles from 7-d chick embryos were dissociated into their component cells by trypsinization (DeHaan, 1967; 1970). The cells were allowed to reaggregate for 24–48 h on a gyratory shaker (Moscona, 1961) in medium 818A (Sachs and DeHaan, 1973) containing 1.3 mM K^+, under an atmosphere of 5% CO_2, 10% O_2, and 85% N_2. The aggregates were allowed to adhere to the bottom of a Falcon plastic tissue culture dish (Falcon Plastic, Oxnard, Calif.) in medium containing 4.5 mM K^+ at 37°C. Nontoxic mineral oil (Klearol, Sonneborn Division, Witco Chemical Corp., New York) layered over the medium prevented evaporation; gas mixture was directed from a toroidal gassing ring over the dish. Under these conditions, aggregates continued beating for hours or even days. The measurements in this study were performed on aggregates made quiescent with 10^{-5} g/ml tetrodotoxin (Calbiochem, San Diego, Calif.).

Measurements of aggregate diameter (range 122–265 μm) were made at a magnification of ×62 with an ocular reticle having a resolution of ~7 μm. The spherical diameter (D) used to represent aggregate size was taken as 2 $(ab)^{1/2}$, where a and b were the major and minor hemiaxes seen from a top view of the preparation. Since 20% of total aggregate volume (V_a) was extracellular space (McDonald and DeHaan, 1973; Elsas et al., 1975; Nathan and DeHaan, 1979),[1] the number of cells (N) per aggregate was calculated from 0.8 V_a/V_c, where cell volume (V_c = 660 μm^3) was derived from a mean cell radius (r_c) of 5.4 μm from freshly dissociated single cells.[2] The total aggregate cell surface was calculated as $4\pi r_c^2 N$. N was also estimated by measuring aggregate DNA content by using an observed value for DNA per cell (Δ_c) of 2.8 × 10^{-12}g in single ventricle cell suspensions and in chicken erythrocytes (Santora et al., 1978). Total DNA per aggregate (Δ_a) was determined by the method of Giles and Myers (1965) from pooled groups of counted and sized aggregates. The mean cell volume calculated from these DNA assays was 651 μm^3, and the values of N determined from Δ_a/Δ_c agreed within ±1% of those calculated from measurements of aggregate diameter. The total membrane area of an aggregate 150 μm in diameter is 7.8 × 10^{-3} cm^2. In calculating membrane area no correction was made for noncardiac cells, which represented about 20% of the aggregate population (Sachs and DeHaan, 1973).

Electrophysiological Measurements

Voltage noise and membrane impedance were obtained by using techniques described earlier (DeFelice and DeHaan, 1977; DeHaan and DeFelice, 1978*a*). Two glass microelectrodes filled with 2 M KCl were inserted into separate cells at distant points within a quiescent aggregate. Electrode resistance was 10–30 MΩ. An 11-mV range (−70 to −59 mV) of transmembrane potentials (V) near rest (E_r) was explored by injecting small positive or negative rectangular current pulses through one of the electrodes.

Noise and pulse data were obtained by amplifying the voltage signal from each electrode separately in two parallel channels: a low gain, field effect transistor input, DC-coupled voltage follower for recording V and voltage responses to current pulses, and a high gain AC-coupled amplifier (3 dB roll-off at 0.015 Hz) to record spontaneous voltage fluctuations around V. Data were stored on FM 7-track tape at 3¾ inches per second (DC, 625 Hz). Injected currents were recorded as the input voltage to a 10^9-Ω resistor.

---

[1]Using electron microscopic stereology, Clapham (1979) has determined that only ~5% of the aggregate volume is extracellular space. Whether these ultrastructural measurements or those using chemical methods are more accurate is not clear at present. However, at worst, this finding would increase our values of R_m and diminish that for C_m by ~12%.

[2]Atherton, B. T., and R. L. DeHaan. Unpublished work.

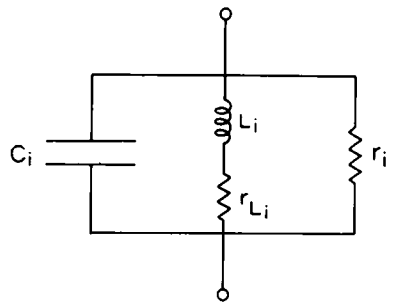

FIGURE 1 The RLC equivalent membrane circuit used for model impedance calculations.

Voltage responses of 1–2 mV amplitude or smaller were obtained with rectangular current pulses typically of 0.1 to 1 nA amplitude. Pulse duration was 4 or 5 s. Each pulse was repeated two or three times for off-line signal averaging.

Pulse Analysis

The recorded voltage pulses were filtered by a simple low pass RC filter with a 3-dB roll-off at 100 Hz. The filtered waveform was further amplified after dialing off V with a variable voltage offset device and was uniformly sampled by an A/D converter at 4-ms intervals. Computer plots of the digitized pulse records were produced on a Tektronix 4010 interactive graphics display terminal and a 4361 hard copy unit (Tektronix, Inc., Beaverton, Oreg.). The theoretical response of the circuit shown in Fig. 1 was fit to the experimental data in accordance with Eqs. 4–6 (below).

Voltage Noise Analysis

Voltage noise records were analyzed with a Hewlett-Packard 3721A correlator (Hewlett-Packard Co., Palo Alto, Calif.) with a high pass RC-filter (3 dB roll-off at 0.1 Hz) at the DC-input. Records of 41 to 110 s were used to produce correlation functions having a lag time of either 1/3 or 1 s. Microelectrode noise was eliminated by cross-correlating the noise signal of the two electrodes to obtain the autocorrelation (C_V) of the inherent voltage noise of the aggregate.

Calculation of Current Noise Parameters

The spectral density $S(f)$ and the correlation function $C(\tau)$ are related by:

$$S(f) = 4 \int_0^\infty C(\tau) \cos \omega\tau \, d\tau \tag{1a}$$

and

$$C(\tau) = \int_0^\infty S(f) \cos \omega\tau \, df. \tag{1b}$$

In this study the voltage noise correlation function C_v was measured experimentally and the membrane impedance Z was determined from the pulse analysis. The current noise spectrum S_I was assumed to be a single Lorentzian, $S_I(\omega) = S_I(0) / (1 + \omega^2\tau_s)$. The corresponding theoretical expression for C_v was determined from $S_v = S_I|Z|^2$ and Eq. 1b. A best fit of this expression to the experimentally determined C_v was obtained by optimizing the parameters $S_I(0)$ and τ_s. $S_I(0)$ could also be obtained from numerical integration of C_V. Since $S_I(0) = S_V(0)/R_i^2$, where R_i is the input slope resistance, Eq. 1*a* gives

$$S_I(0) = (4/R_i^2) \int_0^\infty C_V(\tau) \, d\tau. \tag{2}$$

This method avoided the curve-fitting procedure, and used the noise and pulse data in a more direct way. The curve-fitting process was required, however, to obtain τ_s.

RESULTS

Resting Potential

The resting potentials of the nine aggregates included in this study are given in Table I. The values of E_r fell into two classes: either -64 ± 3 mV or -50 ± 1 mV. Stable membrane voltages (V) away from E_r could be achieved between -70 and -59 mV by injecting current. But steady potentials between -59 and -50 mV could not be maintained. For example, it was possible to hyperpolarize aggregate A-2 (Fig. 2) from $E_r = -50$ mV and hold it at $V = -62$ mV, but with a gradual decrease of the steady hyperpolarizing current V jumped suddenly back to the 50 state. That is, the region between -59 and -50 mV appears to exhibit a negative steady-state slope conductance. The data presented below were therefore all obtained from the voltage range -70 to -59 mV.

Determination of Membrane Electrical Constants

Representative voltage responses to rectangular hyperpolarizing current pulses are shown in Fig. 3 for aggregates of approximately the same size but at different potentials. The slope resistance (R_i) of the aggregate membrane was determined from the steady-state voltage change at the end of such pulses, divided by the injected current (I_0). The responses in Fig. 3 are of nearly the same amplitude for rather different values of I_0; that is, R_i is a sensitive function of V in the -70- to -59-mV potential range. Consequently, very small responses ($\simeq 1$ mV) were required to determine accurately the voltage dependence of the membrane electrical parameters. The on-response to hyperpolarizing pulses was used for the noise and impedance model calculations.

The values of R_i for the aggregates used (Table I) were all significantly greater than the maximal estimate (70 kΩ) for the resistance of the extracellular space (Clapham, 1979). This suggested that the access resistance to the membrane, in aggregates smaller than 250 μm, may be neglected in the model. C_i was determined from the initial portion of the pulse, since the first 40–60 ms of the response was very nearly a straight line with a theoretical slope of I_0/C_i (inset of Fig. 6). Determinations of C_i from the initial slopes of several pulses ($n = 5$–10)

TABLE I
AGGREGATE SIZE, RESTING POTENTIAL, AND INPUT RESISTANCE

Aggregate	D	E_r	R_i
	μm	*mV*	*MΩ*
1	122	−51	6.8
2	125	−49	11.0
3	133	−62	6.1
4	171	−64	4.8
5	190	−65	1.3
6	186	−67	1.2
7	228	−67	0.70
8	247	−66	0.55
9	265	−67	0.35

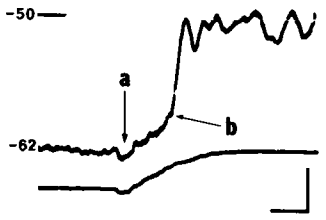

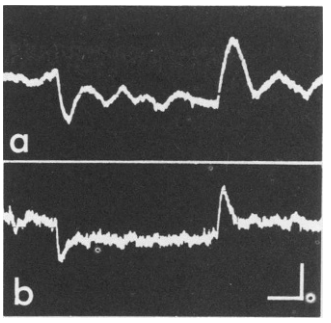

FIGURE 2

FIGURE 3

FIGURE 2 Instability of membrane potential in the range between −50 and −59 mV. Top trace: V from a 125-μm diameter aggregate. At the left side of the figure −1.5 nA current was being passed through the preparation. At (*a*) current is gradually decreased to −1.0 nA. V begins to depolarize in response, but at −59 mV (*b*) it jumps spontaneously to −51 mV. Lower trace: current injected into the aggregate, measured as voltage across the $10^9\Omega$ resistor through which current was passed. Scale 4 mV (trace 1), 0.6 nA (trace 2), 5 s.

FIGURE 3 Voltage responses to rectangular hyperpolarizing current pulses. (*a*) −0.17 nA injected into a 171-μm aggregate, E_r = −61 mV; R_i = 4.2 MΩ; (*b*) −0.70 nA injected into a 190-μm aggregate, E_r = −67 mV; R_i = 0.7 MΩ. Records filtered through a low pass filter flat to 100 Hz. Scale: 1 mV, 1 s.

from the nine aggregates in Table I are plotted in Fig. 4 on a double logarithm scale. (The error bars represent ±SD for each set of observations). A least-squares estimate of the best fit straight line for the unequally weighted data points in Fig. 4 (Guest, 1961) gave a slope of 3.2 ± 0.4 (±SD). This result suggests that C_i is directly proportional to D^3 ($P = 0.70$) or the total membrane surface area in the preparation. If all the cells contribute uniformly to C_i,

$$C_i = C_m N\pi d^2 = 0.8\,\pi d^2\, C_m (D/d)^3. \tag{3}$$

The value of C_m (specific membrane capacitance) calculated from Fig. 4 and Eq. 3 is 1.24 ± 0.18 μF/cm^2. Similarly, measurement of R_i *vs.* D (Fig. 5) at a constant V indicates that R_i is proportional to D^{-3} ($P = 0.75$). That is, R_i is inversely proportional to the total membrane surface area. The specific membrane slope resistance (R_m) for V = −68 ± 2 mV calculated from this result is 18 ± 2.5 kΩ·cm^2. The line drawn through the experimental points in Fig. 5 was derived from the model of Eisenberg et al., 1979 (see Discussion).

The theoretical response of the RLC circuit (Fig. 1) to a current step I_0 is

$$V(t) = R_i I_0\left(1 - \frac{p_1 e^{p_2 t} - p_2 e^{p_1 t}}{p_1 - p_2}\right) + I_0/C_i\left(\frac{e^{p_1 t} - e^{p_2 t}}{p_1 - p_2}\right), \tag{4}$$

where

$$p_1 = 1/2[r_{L_i}/L_i + 1/(r_i C_i)] + 1/2\,\{[r_{L_i}/L_i + 1/(r_i C_i)]^2 - 4(1 + r_{L_i}/r_i)/(L_i C_i)\}^{1/2} \tag{5}$$

or

$$p_1 = -A + \sqrt{B}$$

$$p_2 = -A - \sqrt{B}$$

and

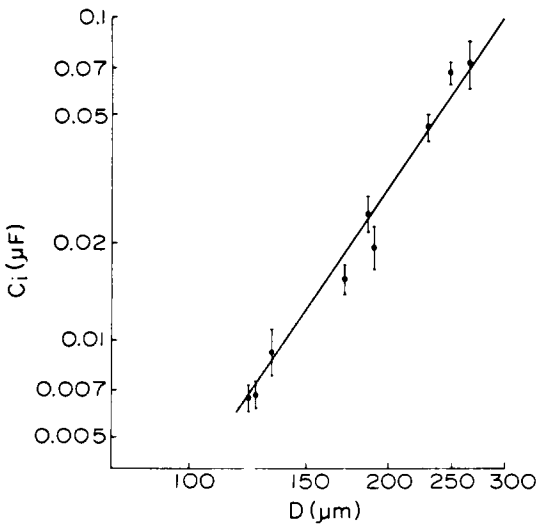

FIGURE 4

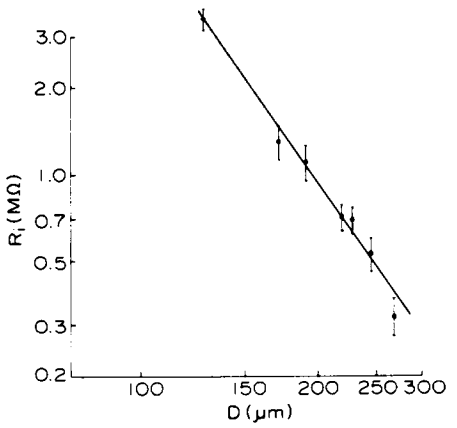

FIGURE 5

FIGURE 4 Input capacitance (C_i) as a function of aggregate diameter (D). C_i measured from the initial slopes of 5–10 pulses from each aggregate. Vertical error bars represent ±SD. Estimate of error for D is ±10 μm. The solid line is the least-squares fit to the data using the relation $C_i \sim D^3$. Log-log scale. C_m = 1.24 ± 0.18 μF/cm².

FIGURE 5 Input resistance (R_i) as a function of aggregate diameter (D) at V = −68 ± 2 mV. Significance of error bar same as in Fig. 3. The solid line was calculated (Clapham, 1979) from the model of Eisenberg et al. (1979) using the following parametric values: R_{int} = 150 Ω·cm, R_{ext} = 600 Ω·cm, ϕ = 60°, f = 0 Hz, r = 0, R = 0.9 (radius), $S/V = 4.4 \times 10^3$ cm^{-1}, $R_m = 1.8 \times 10^4$ Ω·cm².

$$R_i = r_i/(1 + r_i/r_{L_i}). \tag{6}$$

The quantity r_{L_i} is the resistance of the inductive branch in parallel with the capacitor C_i and resistor r_i (Fig. 1). The total membrane surface appears in Eq. 4 only in R_i and C_i. Time constants of the subthreshold response are independent of aggregate size. For example, the time-to-peak voltage of the voltage overshoots, such as those in Fig. 3, should depend only on V and not on D. All of the pulse measurements are consistent with that prediction. All pulse responses were fit by an RLC circuit with a single inductive branch, as shown in Fig. 1, which assumes a single time-dependent conductance in the range −70 to −59 mV.

The parameters r_i, r_{L_i}, and L_i were determined from R_i and from curve-fitting Eq. 4 by eye to the pulse waveform. An example of the results of this procedure is shown in Fig. 6 for the pulse response illustrated in Fig. 3 *a* averaged with a second response to an identical stimulus. All of our responses could be described by this circuit model, indicating that the RLC model in which access resistance was neglected was satisfactory for describing the membrane electrical behavior (see Discussion).

Voltage Dependence of Membrane Circuit Parameters

The membrane resistance increased significantly with depolarization from −70 mV to −59 mV. This is shown in Fig. 7, which represents data from five aggregates of different size. R_m

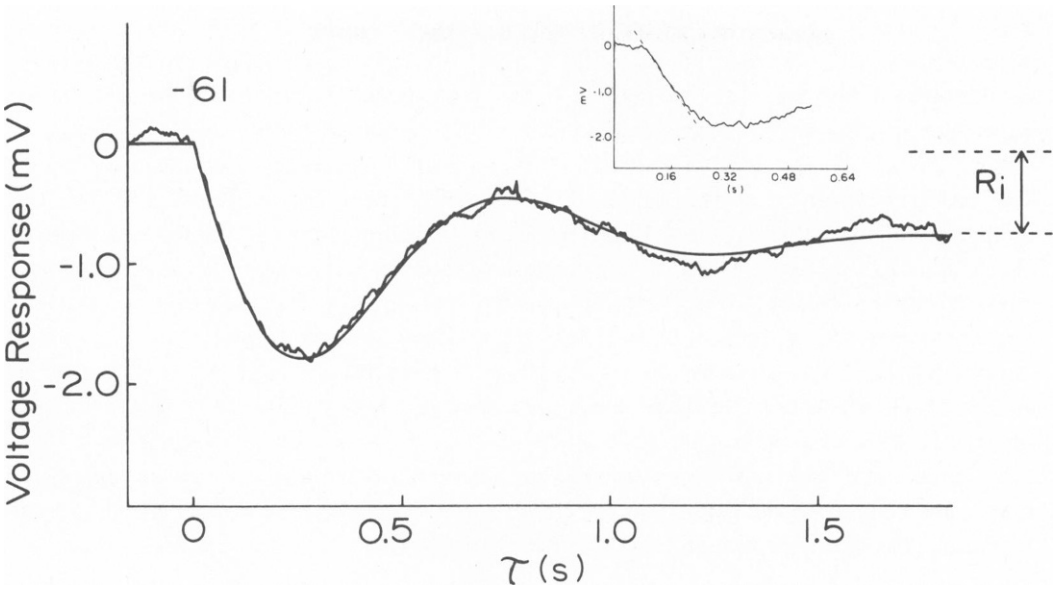

FIGURE 6 Average of two identical voltage pulses (one of which is shown in Fig. 3 *a*) recorded from the same 171-μm diameter aggregate. Theoretical line is the best fit response of the RLC circuit described in the text. Inset: initial portion of one of the pulses, showing how the initial slope was determined in measuring C_i. C_i for this aggregate = 0.015 μF. R_i = 4.8 MΩ, E_r = −61 mV.

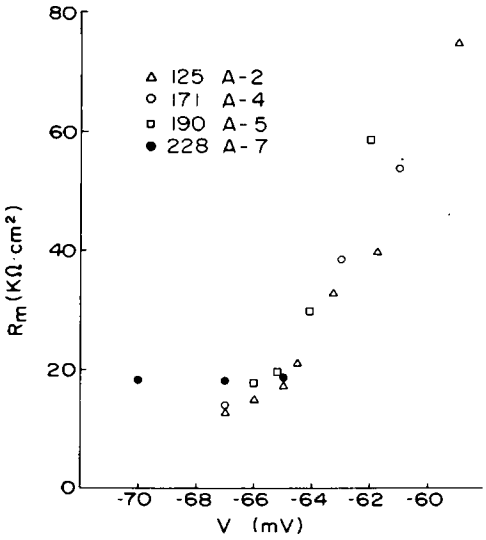

FIGURE 7

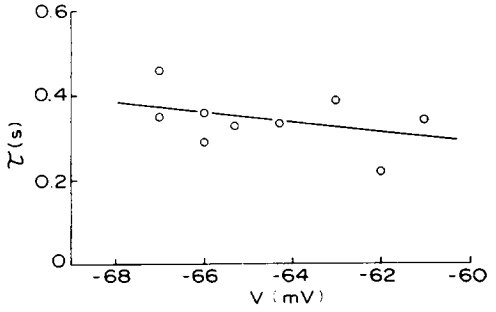

FIGURE 8

FIGURE 7 Voltage dependence of R_m. V = stable potential, either resting or held by steady current. Data are included only for aggregates in which pulses were injected at two or more potentials. Aggregate number (from Table I) and diameter (in micrometers) are given.

FIGURE 8 Time constant of membrane current derived from the comparison of the RLC representation of voltage pulses with an HH-like model conductance ($\tau = L / r_L$). The solid line is the least-squares fit to the data.

was calculated by multiplying the corresponding measurement for R_i by the total membrane surface area. The increase of R_m with V (Fig. 7) represents changes in the parallel combination of the two resistors in Fig. 1, and corresponds mainly to an increase in the parameter r_i. This resistor increases threefold in value from 40 kΩ·cm^2 at $V = -70$ mV to 120 kΩ·cm^2 at -61 mV. The change in the inductor branch parameters was considerably less. The specific resistance of the inductor (r_L) increased from 20 to 30 kΩ·cm^2 and the inductance increased from 25 to 35 kH·cm^2. The ratio of the inductance to the resistance of the inductor (L_i/r_{Li}) is equal to the time constant of the voltage-dependent ionic conductance. Time constants obtained from the pulse analysis are shown in Fig. 8. The time constant appears to be weakly dependent on voltage in the -70- to -59-mV range.

Four representative cross-correlation functions of membrane voltage noise are shown in Fig. 9, *A–D*. These are calculated from noise records obtained simultaneously from two separate cells in an aggregate. One of the noise records is shown in each inset. The cross-correlation functions approximate the autocorrelation function of the aggregate membrane noise, independent of microelectrode noise. The dotted and broken lines represent theoretical fits of the correlation functions (see Discussion).

DISCUSSION

Voltage Stationarity

The long time-scale and narrow voltage range of our observations required impalements of unusual stability. Data for analysis were taken from recordings in which the membrane

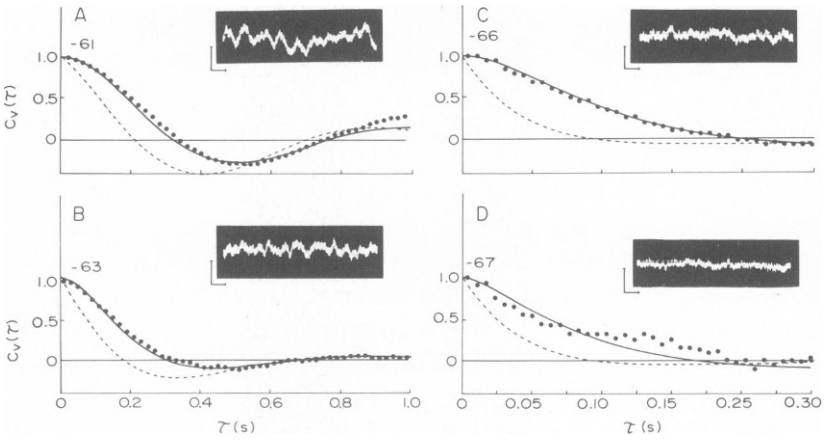

FIGURE 9 Insets: Voltage noise from two aggregates. Left-hand panels are from a 171-μm aggregate (A-4, Table I) at -61 and -63 mV. Right-hand panels are from a 125-μm aggregate (A-2, Table I) at -66 and -67 mV. Vertical and horizontal bars represent 0.60 mV and 1 s, respectively. Main figure: filled circles are $C_V(\tau)$ determined directly from the noise records and normalized. Solid lines are the best fits to the data of the theory described in the text. Maximum lag times are 1 s and 0.30 s for the left- and right-hand panels, respectively. $C_V(0)$ is 3.6×10^{-8} V^2 for $V = -61$ mV, 1.5×10^{-8} V^2 for $V = -63$ mV, 0.45×10^{-8} V^2 for $V = -66$ mV, and 0.24×10^{-8} V^2 for -67 mV. The broken lines are $C_V(\tau/\tau_s)$ in the limit $\tau_s \to 0$, where τ_s is the time constant of the theoretical expression used to fit the data. The τ_s of the best fit lines is 0.45 s for $V = -61$ mV, 0.55 s for $V = -63$ mV, 0.1 s for $V = -66$ mV, and 0.09 s for $V = -67$ mV.

potential remained stable within 0.5 mV for periods of 10–20 min at several different potential levels. Voltage offsets resulting from tip potentials or amplifier drift were negligible in these experiments.

One experimental difficulty intrinsic to the preparation was the occasional nonstationarity of the membrane near −59 mV. The aggregate sometimes produced macroscopic oscillations that either subsided or led to an action potential (DeHaan and DeFelice, 1978*a*). None of the noise records used for final analysis contained these large oscillations.

Voltage Homogeneity

No real system can achieve ideal voltage uniformity since any two spatially distinct points are separated by a finite resistance. Nonetheless, the present results suggest that a lumped circuit model of the total cellular membrane, in which access resistance is neglected, is appropriate for heart cell aggregates of sizes D = 100–250 μm, in the specified frequency and voltage range.

The three-dimensional spread of potential in spherical syncytial systems has been analyzed (Eisenberg and Engel, 1970; Peskoff and Eisenberg, 1975; Eisenberg and Rae, 1976). The recent model of the electrical properties of such a preparation by Eisenberg et al. (1979; the Eisenberg, Barlicon, and Mathias [EBM] model) may be used to derive approximate solutions for the impedance of our heart cell aggregates. Their lumped circuit approximation (EBM, Fig. 6) consists of two parallel RC branches in series with a resistance. The first branch contains the total membrane impedance, as if all the cellular membrane contributed equally; the impedance due to this component varies inversely with D^3. This total membrane area is accessed through a resistive pathway that includes both intracellular and extracellular space; the access resistance varies inversely with D and is independent of frequency. The second branch contains only the outer surface membrane of the sphere; the impedance due to this component varies inversely with D^2. The resistance in series with these two parallel branches results from the point source of current that produces a large local drop of potential essentially independent of frequency; this resistance varies inversely with D.

In Fig. 5 we have shown that the DC-input resistance of our aggregates varies inversely with D^3. The solid line through our data points is the calculated dependence of R_i on D using the EBM model with parameters appropriate to a heart cell aggregate. The line is indistinguishable from a least-squares fit to the data points with slope −3 and specific membrane resistance R_m = 18 k$\Omega \cdot$cm^2. The dependence of impedance on size is insensitive to cleft space between 5–20%, and begins to depart from the linear relationship at frequencies above 10 Hz (Clapham, 1979).

We conclude that of the several terms in the EBM lumped circuit equivalent, the branch representing the total cellular membrane dominates the measured impedance under our experimental conditions. For the heart cell aggregate at potentials near rest, the access resistance and any artifact resulting from a point current source may apparently be neglected. That is, the preparation does not deviate perceptibly from voltage uniformity for signals of frequencies limited by the membrane impedance. This conclusion is confined to a specific set of parameters, the most important factors being high specific membrane impedance, loose cellular packing with a large, well-distributed cleft space, and low frequency signals. For the very different parameters of the frog lens (EBM, 1979), the series resistance term dominates,

and the transmembrane potential varies significantly with distance from a point current source for signals in the range 0–100 Hz.

For the heart cell system the degrading effect of membrane capacitance on voltage uniformity is also countered to a large extent by the inductive component of the membrane impedance; as frequency is increased from DC, the membrane impedance becomes larger up to ~1Hz before it becomes smaller.

Because of the long time-constant of voltage responses to current pulses near rest, our conclusion that cleft resistance is negligible has been tested only in the range 0–10 Hz. The practical result of our conclusion has been to scale all electrical properties of the aggregate, including spontaneous voltage noise, to a standard area equal to the total cellular membrane in the aggregate.

Interpretation of Membrane Inductance

The voltage responses shown in Fig. 2 may be compared with those illustrated in Fig. 23 of the Hodgkin and Huxley (1952) data from the squid giant axon. The small oscillatory responses of the two preparations are qualitatively similar, but the time scale of the heart is about a hundred times longer than nerve. A satisfactory description of this inductive reactance is provided by the Hodgkin and Huxley (HH) model of membrane ionic conductances (Hodgkin and Huxley, 1952; Mauro et al., 1970); the linearized form of the HH equations for a particular current gate is mathematically equivalent to a parallel combination of a resistor and an inductor with an internal resistance. Consider an HH-like model for a capacitive current, a leakage conductance, and one voltage- and time-dependent conductance. The total current for this model is given by

$$I = C\dot{V} + g_1(V - E_1) + \bar{g}s(V - E), \tag{7}$$

where g_1 is the leakage conductance, $\bar{g}$ is the fully activated conductance of the HH-like current, $s(0 < s < 1)$ is the fraction of conductance activated, and E and E_1 are equilibrium potentials. The equation for s is

$$-\dot{s} = -s/\tau_s + \alpha, \tag{8}$$

where τ_s and α are voltage dependent. The small-signal impedance (Z) of the circuit is approximately given by

$$Z^{-1} = \partial I(\omega)/\partial V(\omega) = i\omega C + (g_1 + \bar{g}s_\infty) + \bar{g}(V - E)\left(\frac{\partial \alpha}{\partial V} - s_\infty \frac{\partial}{\partial V}\frac{1}{\tau_s}\right)/(i\omega + 1/\tau_s), \tag{9}$$

where $i = \sqrt{-1}$, $\omega = 2\pi f$ is the radial frequency, and $s_\infty = \alpha\tau_s$; α, τ_s, and their derivatives are evaluated at the reference potential V. The small-signal impedance of the RLC circuit (Fig. 1) is given by

$$Z^{-1} = i\omega C + 1/r + 1/(i\omega L + r_L). \tag{10}$$

A term by term comparison of Eqs. 9 and 10 shows that $r = (g_1 + \bar{g}s_\infty)^{-1}$ and that $L/r_L = \tau_s$. Thus we have interpreted the inductive response to a current step in terms of the activation time constant τ_s. τ_s as a function of V is shown in Fig. 8.

Voltage Noise Analysis

Voltage noise similar to that illustrated in Fig. 9 has been reported in nerve membrane, synthetic lipid bilayers containing macromolecules, and post-synaptic muscle membrane (cf. Neher and Stevens, 1977; DeFelice, 1977, for reviews). Recently, similar noise has been recorded from heart (DeFelice and DeHaan, 1975; Kass et al., 1976; Irisawa and Noma, 1977). These voltage fluctuations are significantly greater than Johnson noise; a rough calculation using a typical chord resistance of 10 MΩ and a bandwidth of 0–10 Hz gives 1.6×10^{-12} V^2, or about 1 μV rms for the Johnson noise amplitude. This is about 3 orders of magnitude less than the noise we normally record. It is generally argued that the mechanism that underlies voltage fluctuations in all membranes is modulation of ion flow through a membrane channel. Current would be regulated by a gate that may either block the channel or allow ions to pass. The time at which opening occurs and the duration of the open state are thought to be random processes. Such a mechanism is supported by observations of discrete, steplike changes in membrane current that occur in bilayers containing gramicidin or other molecules and in chronically denervated, hypersensitive muscle membrane (reviewed by Neher and Stevens, 1977).

The noise properties of this model membrane arise from the kinetics of the individual channels which are described by

$$\left([C] \underset{\beta}{\overset{\alpha}{\rightleftharpoons}} [O]\right),$$

where $[C]$ and $[O]$ are the closed and open states of the ion gates (Fitzhugh, 1965; Hill and Chen, 1972; Stevens, 1972). The parameters α and β are related to probabilities that the channel will instantaneously jump from one state to the other. If the channel is closed at some arbitrary time t, the probability that it will jump to the open state in the infinitesimal time interval $(t, t + dt)$ is αdt. The probability that it will jump to the closed state in $(t, t + dt)$ is βdt. When α is small compared with β, the channel more likely will be in the closed state, and conversely. That is, α^{-1} is the average duration of the closed state of any single channel (τ_c) and β^{-1} is the average duration of the open state (τ_o). The kinetics of the open-close process are described by considering the possible transitions that may occur in the interval $(t, t + dt)$. The probability that a channel is open at time $t + dt$ is written as $p(t + dt)$. The probability that the channel was closed at time t is $1 - p(t)$; the probability that it remained open during the entire interval is $1 - \beta dt$. Therefore,

$$p(t + dt) = \alpha dt[1 - p(t)] + (1 - \beta dt)p(t), \tag{11}$$

or in the limit $dt \to 0$,

$$\dot{p} = \alpha(1 - p) - \beta p. \tag{12}$$

Eq. 12 is identical to Eq. 8 if s is equivalent to p. That is, the macroscopic conductance parameter $s(t)$ may be interpreted on a microscopic scale as representing the probability that a single channel is open at time t. The number of open channels at time t is given by $N_s s$, where N_s is the total number of channels per unit area, both open and closed. Moreover, the steady-state probability that any single channel is open is given by

$$s_\infty = \alpha/(\alpha + \beta) = (1 + \tau_c/\tau_o)^{-1}, \tag{13}$$

and the time constant of the channel is

$$\tau_s = (\alpha + \beta)^{-1} = \tau_o\tau_c/(\tau_o + \tau_c). \tag{14}$$

The correlation function $C(\tau)$ of the random openings and closings of the N_s channels is (Hill, 1968; Hill and Chen, 1972)

$$C(\tau) = N_s s_\infty(1 - s_\infty) \exp(-\tau/\tau_s). \tag{15}$$

The correlation function $C_I(\tau)$ of the fluctuations of current through the N_s channels is

$$\begin{aligned} C_I(\tau) &= N_s\gamma^2(V - E)^2 C(\tau) \\ &= N_s\gamma^2 s_\infty(1 - s_\infty)(V - E)^2 \exp(-\tau/\tau_s) \\ &= I_\infty^2(1 - s_\infty)/(N_s s_\infty) \exp(-\tau/\tau_s), \end{aligned} \tag{16}$$

where γ is the single channel conductance and $I_\infty = N_s\gamma s_\infty(V - E)$ is the steady-state current. The current spectral density $S_I(\omega)$ derived from Eq. 1*a* is

$$S_I(\omega) = 4\,\tau_s\, I_\infty^2(1 - s_\infty)/(N_s s_\infty)[1 + (\omega\tau_s)^2] = S_I(0)/[1 + (\omega\tau_s)^2]. \tag{17}$$

The parameter $S_I(0)$ is useful for testing noise models (Conti et al., 1975, 1976) and is the most reliable measure of our noise data.

The analysis of our noise data was based on Eqs. 17 and 16 and $S_I\,|\,Z\,|^2 = S_V$ (Wanke et al., 1974). $C_V(\tau)$ was determined from each noise record (cf. solid points inFig. 9), and the circuit parameters in Fig. 1 were calculated by fitting pulses immediately preceding or following the noise record to Eq. 4. The membrane impedance was determined from Eq. 10 and the pulse fit values of r_L, r, L, and C. We then determined the theoretical $C_V(\tau)$ from $S_V = S_I\,|\,Z\,|^2$ using Z from Eq 10, S_I from Eq. 17, and the Fourier-transform relation between C_V and S_V in Eq 1*b*. A best fit of this theoretical expression for C_V to the data points for C_V was carried out by optimizing the values for $S_I(0)$ and τ_s. A summary of results for these parameters is given in Fig. 10. The identity between τ_s and $L\,/\,r_L$ was not assumed to hold a priori since the time constant determined from noise data is not the same as the impedance time constant if more than one gating particle modulates ion flow through a channel (Conti et al., 1975). If only one gating particle is involved, the two time constants are the same. Three of the values of τ_s in Fig. 10 are near 0.1 s. The remaining six values are consistent with those derived from the pulse analysis in Fig. 9. The lower values come from a voltage range where the noise is smallest and therefore least reliable. Consequently, we interpret our data as supporting a model in which only one gating particle is involved. This result is supported by recent voltage clamp experiments (Shrier, et al., 1978) that have shown that time-dependent membrane current changes produced by voltage clamp steps in the pacemaker voltage range can be described by a single exponential function.

Interpretation of Results for $S_I(0)$

It is perhaps instructive to express $S_I(0)$ completely in terms of the channel parameters defined above. Eqs. 14, 16, and 17 give

$$S_I(0) = 4\tau_s I_\infty^2[(1 - s_\infty)/N_s s_\infty] = 4N_s\gamma^2(V - E)^2[s_\infty(1 - s_\infty)\tau_o\tau_c/(\tau_o + \tau_c)]. \tag{18}$$

Since s_∞ and $(1 - s_\infty)$ are the steady-state probabilities that any single channel is open or closed, respectively, Eq. 18 is unaffected if the roles of the open and closed states are reversed. If s_∞ decreases with depolarization, $(1 - s_\infty)$ increases. The product $s_\infty(1 - s_\infty)$ is the same in either case.

The value of $S_I(0)$ increases by 10-fold over a 6-mV range (Fig. 10). This increase is apparent from the noise records shown in Fig. 9. Compare Fig. 9 *d* at −67 mV with Fig. 9 *a* at −61 mV. The resistances in these two cases are nearly the same (because of their different sizes) and the noise may be compared directly. A similar increase of $S_I(0)$ with small depolarizations from rest has been reported for squid giant axon (Conti et al., 1975). In nerve this may be explained by an increase in the open-state probability of potassium channels, since the slope resistance decreases with depolarization. The sharp increase of slope resistance with depolarization for our preparation (Fig. 7) suggests that s_∞ decreases with depolarization. As noted, this would also give a sharply increasing value of $S_I(0)$, but would not result in an increase in open channel current (Eq. 18).

An alternative explanation for our observations is offered by a two-current model in which one current is described by a time-dependent channel that opens with depolarization and has a linear, instantaneous current-voltage (IV) relation, and the second current is a time-independent component with negative slope conductance in the voltage range of our observations. The increase in $S_I(0)$ would be explained in this interpretation by the increase in open-state probability of the time-dependent channel with depolarization, coupled with an increase in open-channel current (Eq. 18). The increase in slope resistance is explained by the inwardly rectifying background current. This interpretation is consistent with experimental results from cardiac Purkinje fibers at K_0 = 4–6 mM. McAllister and Noble (1966) demonstrated that Purkinje fibers have both a background current, i_{K_1}, that inwardly rectifies at K_0 = 4 mM, and a time-dependent pacemaker current, i_{K_2} ($\overline{i_{K_2}} \cdot s$) that is activated by depolarization from −90 to −60 mV. At K_0 = 6 mM, i_{K_2} has nearly linear, fully open IV relationship from −100 to −60 mV (Noble and Tsien, 1968). To reconstruct the complete Purkinje fiber action potential McAllister et al., (1975) incorporated these two pacemaker

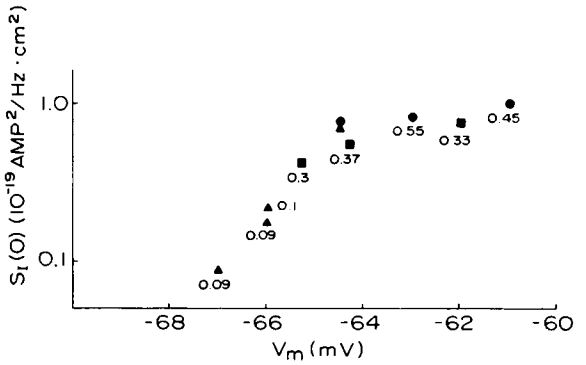

FIGURE 10 Zero frequency current noise amplitude $S_I(0)$ and τ_s calculated from voltage noise and pulse data, as described in the text. The symbols are values for $S_I(0)$ corresponding to the R_m data in Fig. 7. The number next to the symbols is the corresponding value for τ_s (in seconds). The two results for $S_I(0)$ without values for τ_s were determined directly from $C_V(\tau)$ and R_i (Eq. 2).

currents plus 7 other specific conductances in a theoretical framework (the McAllister, Noble, and Tsien [MNT] model) based on extensive voltage clamp analyses and a review of all earlier models. Recent voltage clamp analysis of 7-d embryo ventricular aggregates suggests that this preparation also exhibits two outward currents in the pacemaker voltage range with certain similarities to i_{K_1} and i_{K_2}.[3] A model that includes the i_{K_1} and i_{K_2} components of the MNT reconstruction, with the fully open IV relationship of the i_{K_2} channel corresponding to $K_0 = 6$ mM (Noble and Tsien, 1968) would be qualitatively consistent with both the noise and impedance properties of aggregates in the present paper, and the recent voltage clamp measurements on this preparation (see footnote 3).

The noise and impedance data reported here are sufficient to eliminate a two-current model consisting of a linear background current and $i_{K_2} = \overline{i_{K_2}} \cdot s$, where the increases in both noise and impedance are ascribed to i_{K_2}. If s is activated by depolarization, as in the MNT model, our noise results require that the potential must lie in the activation range of the i_{K_2} channel where $0 < s_\infty < \frac{1}{2}$. However, our impedance results require that the sum of $\overline{i_{K_2}} s_\infty$ and the background current must have a decreasing slope conductance over this potential range. This requirement is satisfied only if $\overline{i_{K_2}}$ is a decreasing function of membrane potential. That is, the fully open channel must have a negative slope conductance region. Since $S_I(0)$ is proportional to $\overline{i_{K_2}}^2 \tau_s s_\infty (1 - s_\infty)$, a decrease in $\overline{i_{K_2}}$ would strongly offset the increase in $\tau_s s_\infty (1 - s_\infty)$ over the potential range for which s_∞ increases from 0 to $\frac{1}{2}$. That is, the noise and impedance data present conflicting requirements on $\overline{i_{K_2}}$. We have been unable to find a theoretical form for this function alone that adequately described both aspects of the results. As mentioned above, this problem is solved by ascribing a voltage dependence to the background current that produces inward rectification with negative slope conductance.

In sum, the most readily apparent interpretation of our data is that over the voltage range stated, the 7-d embryonic ventricle cell membrane exhibits two outward pacemaker currents. One is a nongated background current that inwardly rectifies with depolarization. The other is a gated, time-dependent channel that opens with depolarization and has a linear, or nearly linear, instantaneous IV relation.

$S_I(0)$ may, in principle, be measured directly under voltage clamp over a wider range of voltages than achieved in the present study. Our first attempts at this direct approach were unsuccessful, probably because the amplitude of the current noise is small compared with the noise produced by the voltage clamp circuit. From the maximal value of $S_I(0)$ of 10^{-19} $A^2/Hz \cdot cm^2$ (Fig. 10), the 10-Hz bandwidth of our measurements, and the aggregate surface of 10^{-2} cm^2, the calculated rms current noise $\simeq 10^{-10}$A. Current of such a small magnitude in such a low frequency range may be difficult to measure directly by the two-microelectrode clamp technique. Cross-correlation techniques can eliminate extraneous noise of the microelectrodes (Methods), but these techniques have not been applied successfully to voltage clamp measurements of $S_I(0)$. Direct measurements of $S_I(f)$ have been made using microelectrodes on drug-induced currents at the neuromuscular end plate (Neher and Stevens, 1977) and on the transient inward current in Purkinje fiber (Kass et al., 1976), but not on the voltage-controlled conductances that underlie spontaneous excitability.

[3]Clay, J. R., and A. Shrier. Unpublished work.

Comparison with Other Studies

The impedance measurements in this study differ somewhat from previous work on the chick heart cell aggregate. Our value of 18 $k\Omega \cdot cm^2$ for R_m at $V \cdot -70$ mV is greater than the value of (13 $k\Omega\gamma \cdot cm^2$) reported by DeHaan and Fozzard (1975), presumably because greater attention was given here to the stability of the impalements and the exact potential at which R_i was measured. The sharp increase in R_m with depolarization in a cultured embryonic heart cell preparation has also been observed by Sachs (1976) and is similar to that calculated for the MNT model of the cardiac Purkinje fiber (McAllister et al., 1975). As found previously (DeHaan and DeFelice, 1978*a*), within the strict limits of voltage and frequency, the internal potentials of the cells in TTX-treated aggregates do not deviate appreciably from isopotentiality. This result is a consequence of the high specific membrane impedance, close coupling, and the relatively loose packing of the cells.

The primary difference between our results and studies of other cardiac preparations is our finding that an inductance is required to describe fully the response of the membrane. We have discussed elsewhere the concept that rhythmic firing arises from two distinguishable membrane properties (DeHaan and DeFelice, 1978*a*, *b*): the RLC-like impedance with an inherent resonant frequency, and an intrinsic fluctuation that results from the random opening and closing of individual channels. In the present work, we have calculated values for the parameters of the RLC circuit and have estimated those of the intrinsic noise generator. Small-signal impedance and noise analysis may be used to study oscillatory phenomena in the membrane independent of the full action potential currents. Application of these techniques to aggregates prepared from earlier and later embryonic hearts should lead to greater understanding of how the fundamental electrical properties of cardiac cell membrane develop.

This work was supported by National Institutes of Health grants HL 16567, HL 05346, and HL 17827.

Received for publication 30 November 1978 and in revised form 20 June 1979.

REFERENCES

CLAPHAM, D. E. 1979. A whole tissue model of heart cell aggregates: Electrical coupling between cells, membrane impedance and the extracellular space. Doctoral dissertation, Emory University, Atlanta.

CONTI F., L. J. DEFELICE, and E. WANKE. 1975. Potassium and sodium ion current noise in the membrane of the squid giant axon. *J. Physiol. (Lond.).* **248**:45–82.

CONTI, F., B. HILLE, B. NEUMCKE, W. NONNER, and R. STAMPFLI. 1976. Measurements of the conductance of the sodium channel from current fluctuations at the node of Ranvier. *J. Physiol. (Lond.).* **262**:699–727.

DEFELICE, L. J. 1977. Fluctuation analysis in neurobiology. *Int. Rev. Neurobiol.* **20**:169–208.

DEFELICE, L. J., and R. L. DEHAAN. 1975. Voltage noise and impedance from heart cell aggregates. *Biophys. J.* **15**:130*a*. (Abstr.).

DEFELICE, L. J., and R. L. DEHAAN. 1977. Membrane noise and intercellular communication. *Proc. IEEE Spec. Issue Biol. Signals* **65**:796–799.

DEHAAN R. L. 1967. Regulation of spontaneous activity and growth of embryonic chick heart cells in tissue culture. *Dev. Biol.* **16**:216–249.

DEHAAN R. L. 1970. The potassium sensitivity of isolated embryonic heart cells increases with development. *Dev. Biol.* **23**:226–240.

DEHAAN R. L., and L. J. DEFELICE. 1978*a*. Oscillatory properties and excitability of the heart cell membrane. *In* Theoretical Chemistry: Advances and Perspectives. H. Eyring, editor. Academic Press, Inc., New York **4**:181–233.

DEHAAN, R. L., and L. J. DEFELICE 1978*b*. Electrical noise and rhythmic properties of embryonic heart cell aggregates. *Fed. Proc.* **37**:8–14.

DEHAAN, R. L., and H. A. FOZZARD. 1975. Membrane response to current pulses in spheroidal aggregates of embryonic heart cells. *J. Gen. Physiol.* **65**:207–222.

DEHAAN, R. L., and H. G. SACHS. 1972. Cell coupling in developing systems: the heart cell paradigm. *Curr. Top. Dev. Biol.* **7**:193–228.

EISENBERG, R. S., and E. ENGEL. 1970. The spatial variation of membrane potential near a small source of current in a spherical cell. *J. Gen. Physiol.* **55**:736–757.

EISENBERG, R. S., and J. L. RAE. 1976. Current-voltage relationships in the crystalline lens. *J. Physiol. (Lond.).* **262**:285–300.

EISENBERG, R. S., V. BARCILON, and R. T. MATHIAS. 1979. Electrical properties of spherical syncytia. *Biophys. J.* **25**:151–180.

ELSAS, L. J., F. B. WHEELER, D. J. DANNER, and R. L. DEHAAN. 1975. Amino acid transport by aggregates of cultured chicken heart cell. *J. Biol. Chem.* **250**:9381–9390.

FITZHUGH, R. 1965. A kinetic model of the conductance changes in nerve membrane. *J. Cell Comp. Physiol.* **66**:111–115.

GILES, K. W., and A. MEYERS. 1965. An improved Diphenylamine method for the estimation of deoxyribonucleic acid. *Nature (Lond.).* **206**:93.

GUEST, P. G. 1961. Numerical Methods of Curve Fitting. Cambridge University Press, J. Wright and Sons, Ltd., Bristol, England.

HILL, T. L. 1968. Thermodynamics for Chemists and Biologists. Addison-Wesley Publishing Co., Inc., New York.

HILL, T. L., and Y. CHEN. 1972. On the theory of ion transport across the nerve membrane. IV. Noise from the open-close kinetics of K Channels. *Biophys. J.* **12**:948–959.

HODGKIN, A. L., and A. F. HUXLEY. 1952. A quantitative description of membrane current and its application to conduction and excitation in nerve. *J. Physiol. (Lond.).* **117**:500–544.

IRISAWA, H., and A. NOMA. 1977. Miniature fluctuations of the membrane potential in the rabbit sinoatrial node cell. *Proc. 27th Int. Cong. Physiol Sci. (Paris).* 345. (Abstr.)

KASS, R. S., S. J. LEDERER, and R. W. TSIEN. 1976. Current fluctuations in strophanthidin-treated cardiac Purkinje fibres. *Biophys. J.* **16**:2*a*. (Abstr.).

MAURO, A., F. CONTI, F. DODGE, and R. SCHOR. 1970. Subthreshold behavior and phenomenological impedance of the squid giant axon. *J. Gen. Physiol.* **55**:497–523.

MCALLISTER, R. E., and D. NOBLE. 1966. The time and voltage dependence of the slow outward current in cardiac Purkinje fibres. *J. Physiol. (Lond.).* **186**:632–662.

MCALLISTER, R. E., D. NOBLE, and R. W. TSIEN. 1975. Reconstruction of the electrical activity of cardiac Purkinje fibres. *J. Physiol. (Lond.).* **251**:1–59.

MCDONALD, T. F., and R. L. DEHAAN. 1973. Ion levels and membrane potential in chick heart tissue and cultured cells. *J. Gen. Physiol.* **61**:89–109.

MOSCONA, A. 1961. Rotation-mediated histogenetic aggregation of dissociated cells. *Exp. Cell. Res.* **22**:455–475.

NATHAN, R. D., and R. L. DEHAAN. 1979. Voltage clamp analysis of embryonic heart cell aggregates. *J. Gen. Physiol.* **73**:175–198.

NEHER, E., and C. F. STEVENS. 1977. Conductance fluctuations and ionic pores in membranes. *Annu. Rev. Biophys. Bioeng.* **6**:345–381.

NOBLE, D., and R. W. TSIEN. 1968. The kinetics and rectifier properties of the slow potassium current in cardiac Purkinje fibres. *J. Physiol. (Lond.).* **195**:185–214.

PESKOFF, A., and R. S. EISENBERG. 1975. The time dependent potential in a spherical cell using matched asymptotic expansions. *J. Math. Biol.* **2**:277–300.

SACHS, F. 1976. Electrophysiological properties of tissue cultured heart cells grown in linear array. *J. Membr. Biol.* **28**:373–399.

SACHS, H. G., and R. L. DEHAAN. 1973. Embryonic myocardial cell aggregates: volume and pulsation rate. *Dev. Biol.* **30**:233–240.

SANTORA, A., F. B. WHEELER, R. L. DEHAAN, and L. J. ELSAS. 1978. Relationship of insulin binding to amino acid transport by cultured 14-day embryonic chick heart cells. *Endocrinology.* **104**:1059–1068.

SHRIER, A., J. R. CLAY, and R. L. DEHAAN. 1978. Voltage clamp analysis of membrane currents at subthreshold potentials in embryonic heart cell aggregates. *Physiologist.* **21**:110. (Abstr.)

STEVENS, C. F. 1972. Inferences about membrane properties from electrical noise measurements. *Biophys. J.* **12**:1028–1047.

WANKE, E., L. J. DEFELICE, and F. CONTI. 1974. Voltage noise and current noise in space clamped squid giant axon. *Pflug. Arch. Eur. J. Physiol.* **347**:63–74.